Dynamic Mode Decomposition Based Epileptic Seizure Detection from Scalp EEG

MUHAMMAD SOHAIB J. SOLAIJA[ID], **(Student Member, IEEE),**
SAJID SALEEM[ID], **(Member, IEEE), KHAWAR KHURSHID**[ID],
SYED ALI HASSAN[ID], **(Senior Member, IEEE),**
AND AWAIS MEHMOOD KAMBOH[ID], **(Senior Member, IEEE)**

School of Electrical Engineering and Computer Science, National University of Sciences and Technology (NUST), Islamabad 44000, Pakistan

Corresponding author: Syed Ali Hassan (ali.hassan@seecs.edu.pk)

ABSTRACT Reliable detection of the onset of epileptic seizures has seen renewed interest over the past few years, owing to several factors including, the global push toward digital health-care, the advancements in signal processing techniques, and the increased computational power of machines. A reliable automatic system could result in tremendous improvement in the quality of life of epilepsy patients. This paper presents dynamic mode decomposition (DMD), a data-driven dimensionality reduction technique, originally used in fluid mechanics, as an instrument for epileptic seizure detection from scalp electroencephalograph (EEG) data. DMD is employed in this paper to measure power of signals in different frequency bands. These subband-powers, along with signal curve lengths, are used as features for training random under-sampling boost decision-tree classifier. Post-processing measures ensure an acceptable balance between false positives and true positives. The proposed algorithm has been tested over a thousand hours of EEG data from two different data sets, the CHB-MIT data set and the KU Leuven data set, giving sensitivity values of 0.87 and 0.88, respectively, and specificity values of 0.99 for both the data sets.

INDEX TERMS Biomedical signal processing, EEG, epileptic seizure detection, dynamic mode decomposition, RUSBoost, decision trees.

I. INTRODUCTION

Epilepsy is one of the most common neurological diseases in the world affecting more than 50 million individuals [1]. There are multiple methods of measuring brain activity, both invasive and non-invasive. This article is limited to the scalp Electroencephalography (EEG), which is a non-invasive, and thus a universally accessible procedure. EEG is the primary diagnostic tool for epilepsy and is most frequently used for epileptic seizure onset detection. This is essentially due to its good resolution in space-time as compared to other techniques.

EEG tests measure the electrical activity generated by brain using metal electrodes placed in a standard configuration on the scalp [2]. Manifestations of epileptic activity can be spatially localized, or generalized, thus necessitating the use of a large number of electrodes for proper monitoring. Since EEG measurements are high-dimensional, spatially and temporally, an automated algorithm for seizure detection would potentially be very helpful to the clinicians. This is especially relevant when certain patients have to under-go long-term EEG tests, ranging from 3 to 5 days at a time.

Another problem in seizure onset detection is the subjectivity of the clinician analyzing the recordings. The clinicians may often disagree on seizure regions in EEG recordings. It has been shown that when experts were asked to review EEG records already marked independently by another expert, just below 80% were marked similarly by two or more experts [3]. To provide consistency in marking the long-term recordings, it is necessary to have automated or semi-automated algorithms mark the regions of interest in the recording, and provide a second opinion to the clinician. With the renaissance of machine learning, and significant advancements in the computational ability of electrical machines, solutions are now possible that provide consistent results over long durations of high-dimensional data.

In this paper, we introduce a technique that originated from the domain of fluid mechanics, called dynamic mode decomposition (DMD), and apply it to EEG signals for detection of

epileptic seizures. The DMD is a data-driven dimensionality reduction technique. We demonstrate the versatility of the algorithm, and its ability to provide reliable and consistent results by testing it over two well-known EEG datasets. The results show that DMD combined with curve-length, has a comparable performance to some of the best performing existing methods used in seizure detection. The sequence of the paper is as follows. Sect. II discusses the recent works carried out using dynamic mode decomposition and various seizure detection algorithms developed and tested on the CHB-MIT and KU Leuven datasets. Sect. III gives a brief description of dynamic mode decomposition followed by presentation of our methodology in Sect. IV. Results are presented in Sect. V and the conclusions are drawn in Sect. VI.

II. RELATED WORKS

Although EEG-based epileptic seizure detection had been studied earlier [4], [5], the field received a boost by the publication of publicly accessible dataset by Massachusetts Institute of Technology collected at Children's Hospital Boston (CHB-MIT dataset) in 2009 by Shoeb and Guttag [6] through Physionet data bank [7]. The dataset, containing 982 hours of EEG recordings from 24 patients, has since been used by the research community as a benchmark for epileptic seizure detection and performance comparison. The work by Shoeb and Guttag [6] was one of the first to use machine learning for seizure detection from scalp EEG. The technique involves derivation of features from signal energy in fixed frequency bands, and use support vector machine (SVM)-based patient-specific classifiers to determine the presence of seizures. Over the years, several innovative and potentially capable techniques and algorithms have been published. However, there have been inconsistencies across studies in the use of the whole, or subset of the dataset, and in the use of performance metrics for evaluation, making it impossible to compare the techniques in an objective manner.

Chiang *et al.* [8] presented an on-line re-training method combined with simple post-processing. The feature set includes phase of the signal at different frequency bands obtained by wavelet decomposition, and the synchronization between pairs of channels. However, this work was validated on only seven patients from the dataset with further limitations on usable data. The approach requires an inter-ictal state of at least 4 hours between two seizures and also the recording should not be disrupted by over an hour. Another patient specific algorithm is proposed in [9] that uses temporal and spectral features to build collective network of binary classifier ensemble (CNBC-E) by employing multi-dimensional particle swarm optimization (MD-PSO) [10]. This algorithm only considers EEG records containing one or more seizures and excludes two patients from the study. Wavelet decomposition has been used extensively for feature extraction from EEG signals [11]–[14]. One approach is to use time-domain statistical quantities like energy, entropy, standard deviation, etc in conjunction with inter-quartile range and mean absolute deviation of raw data as features for a classifier to provide

an accurate and low-latency seizure detection solution. However, this work does not report the false alarm rate or specificity of the algorithm [11].

Absence seizures are detected in [12] by reducing the wavelet basis using principal component analysis (PCA) and then feeding these components into different classifiers. This study uses about only 1% of the entire dataset. The approach proposed in [13] uses wavelet decomposition to split the signal into various sub-bands. The features used were magnitude, spectral energy variation, and morphology of the signal for all the sub-bands. SVMs and extreme learning machines (ELMs) were used for classification. The study leaves out one patient from the dataset without mentioning the patient number and the reason for rejection. A multi-variate extension of empirical wavelet transform is proposed in [14] where features are calculated for automatically selected channels. The authors have excluded patient 12 of the CHB-MIT dataset from their study citing inability to read the EEG for that particular patient. Furthermore, only those EEG recording are considered that contain seizures.

An unsupervised feature learning technique is proposed in [15] that uses multiple layers of single-layer neural networks (auto-encoders) with each layer feeding its output to the next. The stack of auto-encoders (SAE) learns features by setting the target value equal to the input. The features learned by SAE are then fed to patient-specific logistic classifiers. The results of this paper are calculated over only 44 hours of EEG data from 6 patients. A recent unsupervised technique uses group invariant scattering for feature extraction from the EEG data and proposes an anomaly-detection based algorithm for identifying seizure regions [16].

Fergus *et al.* [17] compare performance of various classifiers using power spectral density (PSD), peak frequency, median frequency, root mean-squared (RMS) value, entropy, correlation, skewness, and kurtosis as features. This study also employs a small part of the dataset, i.e., 342 minutes of data only.

Fuzzy entropy (FuzzyEn) is used for seizure detection in [18]. FuzzyEn is calculated from the EEG signals for different epileptic states. The selected features are then used to train SVMs. The authors only consider the data from 18 patients, discarding the others citing lack of data integrity.

A patient-specific seizure detection algorithm is presented in [19] that represents the data in high dimensional phase space. The dimensionality of data is reduced by PCA and Poincaré section is applied to extract features, which are then used to train a two-layered classifier comprising linear discriminant analysis (LDA) and Naive-Bayesian classifiers. The study excludes Patient 15 and only considers EEG records containing seizures.

Closed loop systems for seizure detection have been proposed in [20] and [21]. The former uses phase/amplitude lock values to differentiate between seizure and non-seizure activities of the brain, but only reports its performance for 10 patients. The latter presents an on-chip, patient-specific, dual-detector architecture comprising two linear SVMs.

It uses 600 seconds of pre-ictal, ictal and post-ictal EEG patterns for training of SVM but requires offline extraction of patient specific parameters.

Another scalp EEG dataset has been collected and analyzed at KU Leuven, where Hunyadi *et al.* [22] used features such as signal power at different frequency bands, asymmetry of contra-lateral channel pairs, presence of spikes, and repetitive spikes with evolution in amplitude.

Single channel intra-cranial dataset made available by the University of Bonn [23] has also been considered in a number of studies [24]–[35]. Empirical mode decomposition has been used to compute intrinsic mode functions, whose amplitudes and instantaneous frequencies are employed as features to distinguish between seizure free and seizure regions in the EEG records [24]–[27]. Similarly, a fractional linear prediction model for EEG signal is proposed in [28]. The prediction error and the signal energy are used as features to train the SVM that detects the seizures. Automatic detection of epileptic seizures has been proposed using computation of local binary pattern of EEG signal at stable key points [29]. The points are detected after a multi-scale analysis of the EEG signal. Time-frequency representations for non-stationary signals such as wavelet transform [30]–[34], and eigenvalue decomposition of Hankel matrix, constructed from the observed signal [35], has been very effectively used to detect seizures from single-channel intra-cranial EEG signals. In this paper, we consider the CHB-MIT and KU LEUVEN datasets, which consist of multiple channels of scalp EEG, and apply a spatio-temporal analysis technique (presented in next section) for the detection of epileptic seizures.

III. DYNAMIC MODE DECOMPOSITION

Dynamic mode decomposition (DMD) was developed for flow analysis of fluids [36]. The assumption behind this technique is the existence of a low-dimensional structure underlying otherwise high-dimensional measurements. DMD has been used to analyze the time-resolved particle image velocimetry (PIV) measurements of unforced and harmonically forced gas jets [37]. Different variants of DMD have been developed since [38]–[41]. Brunton *et al.* [42] demonstrate the robustness of DMD to additive Gaussian noise and down-sampling of the signals.

The authors apply DMD algorithm on neural recordings for known motor tasks before combining DMD with clustering algorithms for sleep spindle detection. To the best of our knowledge, our paper is the first time that the DMD has been applied to scalp EEG signals.

Dynamic mode decomposition (DMD) is, in essence, a data-driven dimensionality reduction technique. It relies on the experimental snapshots to make sense of the inherent structure of data instead of using complex mathematical equations or models that govern the behavior of the system. This approach is best suited to problems involving high-dimensional data where either no underlying model exists, or the model is too complex to be validated [43]. For this reason, DMD is a potent candidate as a feature-extraction technique for EEG data as it exploits the low-dimensional structure of the experimental data. The DMD algorithm was initially proposed by [44] and further developed by [36] and [40].

Let $\mathbf{x_j}$ be a column vector containing measurements from n channels at time instant j. Then $\mathbf{X}$ is $n \times m$ data matrix constructed by horizontal concatenation of these measurement vectors for m consecutive time instances, i.e.,

$$\mathbf{X} = \begin{bmatrix} \mathbf{x_0} & \mathbf{x_1} & \dots & \mathbf{x_{m-1}} \end{bmatrix}.$$

Similarly, define $\mathbf{X}'$ as the data matrix containing observation vectors from time instant $t = 1$ to $t = m$, i.e.,

$$\mathbf{X}' = \begin{bmatrix} \mathbf{x_1} & \mathbf{x_2} & \dots & \mathbf{x_m} \end{bmatrix}.$$

Dynamic mode decomposition relies on the assumption that there is a linear operator $\mathbf{A}$ such that

$$\mathbf{X}' = \mathbf{A}\mathbf{X}. \tag{1}$$

Estimating this transition matrix $\mathbf{A}$ enables us to determine a linear regression based relationship between consecutive data matrices ($\mathbf{X}$ and $\mathbf{X}'$). One possible approach for determining this operator $\mathbf{A}$ is to compute the pseudo-inverse of $\mathbf{X}$, however, as we are dealing with high-dimensional data, this may not be computationally convenient [42]. Using our assumption of some low-dimensional structure behind the extensive data, we instead compute a low-rank approximation $\tilde{\mathbf{A}}$ of $\mathbf{A}$ and its eigen-decomposition using the following DMD algorithm.

A. DMD ALGORITHM

The DMD algorithm is defined in [40], and can be presented as following sequence of steps:

1) Find the singular value decomposition (SVD) of the first data matrix $X = U\Sigma V^*$ and substitute into (1) to get $X' = AU\Sigma V^*$.
2) Define $\tilde{A} = U^*AU = U^*X'V\Sigma^{-1}$
3) Find the eigen-decomposition of $\tilde{A}$:
   $\tilde{A}W = W\Lambda$,
   where W is the matrix of eigenvectors and Λ is the diagonal matrix of DMD eigenvalues λ_i.
4) Compute the DMD modes of the data matrix X as follows:

$$\Phi \approx X'V\Sigma^{-1}W \tag{2}$$

Each column of Φ is a DMD mode ϕ_i corresponding to the eigenvalue λ_i.

This allows us to represent the observed data as a composition of coupled spatio-temporal modes, i.e., $\hat{\mathbf{X}}$, the approximation of matrix $\mathbf{X}$ can be represented as

$$\hat{\mathbf{X}} = \Phi exp(\Omega t)\mathbf{z}, \tag{3}$$

where $\Omega = log(\Lambda)/\Delta t$, Δt is the time difference between consecutive snapshots, and $\mathbf{z}$ represents the weights calculated for the first time instant such that $\mathbf{x_0} = \Phi\mathbf{z}$ [42]. The
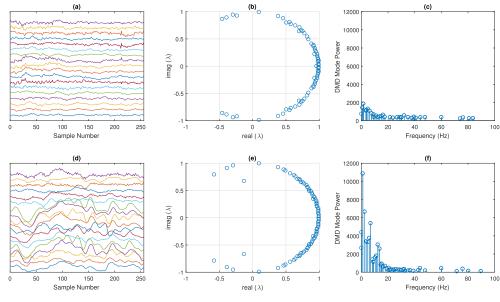
FIGURE 1. Comparison of Eigenvalues and DMD Modes For Seizure and Non-Seizure waveforms (a) Waveform of a one-second long seizure-free EEG recording, (b) Eigenvalues of the waveform shown in (a), (c) DMD mode powers of the waveform shown in (a), according to the method presented in section III-A, (d) Waveform of a one-second long seizure EEG recording, (e) Eigenvalues of the waveform shown in (d), (f) DMD mode powers of the waveform shown in (d).

DMD mode powers are defined as the square of its vector magnitude, i.e.,

$$P_i = |\phi_i|_2^2. \tag{4}$$

As identified in [42], the spatial resolution for neurological signals is usually less than the temporal resolution, e.g., a typical EEG acquisition system may have around 20 scalp electrodes sampling at 256 Hz. This disparity in resolution results in less number of dynamical modes than required to fully capture the dynamics of the neurological activity. Thus, a modification to the standard DMD algorithm (as presented above) is adopted to augment the data matrix **X** by stacking h number of consecutive observation vectors x_j such that the number of rows in **X** becomes at least twice the number of columns. The data augmentation artificially inflate the spatial resolution of data. The details of the data augmentation procedure are presented in [42].

To demonstrate the effectiveness of DMD in discriminating between seizure and non-seizure portions of EEG recording, we have computed the eigen-values of the transition matrix **A** and the power of the resulting spatio-temporal modes Φ for an example EEG data representative of both seizure and non-seizure regions. Fig. 1 illustrates the variation in eigenvalues and DMD mode powers for these example data regions. This example uses 18 channel EEG data of 1-sec duration (for each region) for patient 1 of CHB-MIT dataset, recorded at a sampling rate of 256Hz. Thus the data matrix **X** contains 256 columns and 529 rows. The eigenvalues computed at step 3 of the DMD algorithm are plotted in the complex plane with their magnitude indicating the strength of the mode and the angle representing the frequency, e.g., the angle

from 0 to π radians (first two quadrants) covers the frequency range from 0 to half the sampling frequency, i.e., 128 Hz. The phase of eigenvalues can be converted to frequency (Hz) by the following equation

$$f_i = |imag(\omega_i)/2\pi|, \tag{5}$$

where $\omega_i := log(\lambda_i)/\Delta t$ are the diagonal elements of matrix Ω and $imag(.)$ is the imaginary part of a complex number. The eigen-values occur in conjugate pairs for the real-valued data matrix X.

It can be seen in Fig. 1 that seizure and non-seizure regions differ from each other in terms of both the number of modes and their relative strength in various sub-bands of frequency. For example, the seizure region has greater number of modes and cumulative power in the 0-15 Hz range as compared to the non-seizure region. Also seizure region exhibits lesser number of modes in the 60-128 Hz band.

IV. PROPOSED METHODOLOGY

The overall methodology used for seizure detection in this study is depicted in Fig. 2, and follows the standard sequence of preprocessing, feature extraction, classification, and post-processing. Each of these steps is explained below.

A. PREPROCESSING

Preprocessing ensures that all subjects have the same recording conditions. Thus, for CHB-MIT dataset a total of 18 channels that were present in all patients were selected for processing. These channels include: C3-P3, C4-P4, CZ-PZ, F3-C3, F4-C4, F7-T7, F8-T8, FP1-F3, FP1-F7, FP2-F4, FP2-F8, FZ-CZ, P3-O1, P4-O2, P7-O1, P8-O2, T7-P7 and
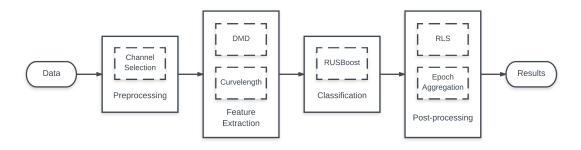
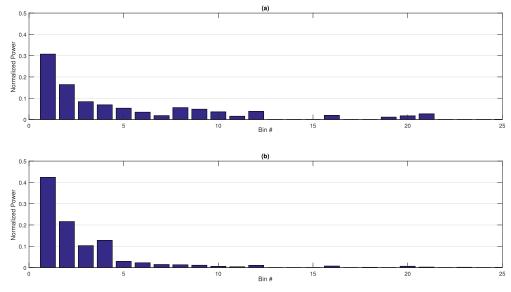**FIGURE 2.** Block Diagram of the Proposed Methodology.

FIGURE 3. (a) Normalized DMD Mode Power for non-seizure epoch shown in Fig 1a, (b) Normalized DMD Mode Power for seizure epoch shown in Fig 1d.

T8-P8. To keep the analysis consistent across subjects, recordings from Patient 12 were removed from analysis because of a different channel configuration. Some recordings of the patient have channels that are entirely different from the 18 channels that were common in all other patients.

All subjects from KU Leuven had the same 22 channels (including ECG) in their recordings, thus no channel selection was required.

The recordings were divided into non-overlapping epochs of one second each. Each epoch is then processed independently until the post-processing stage.

B. FEATURE EXTRACTION

The features used in the proposed approach are the powers of the DMD modes and the curve-lengths of the time-domain EEG signal. The detailed methodology of feature extraction is explained below.

The DMD mode powers were calculated employing the data augmentation approach of [42]. A hard threshold on the singular values was applied in accordance with [45] to retain only the principal spatio-temporal modes. This helps in reducing the number of features and consequently, the training requirements and the computational complexity of the approach. The DMD powers were combined in frequency bins of width 4 Hz, spanning from 0 Hz to half the sampling frequency, i.e., 128Hz. The bins are then normalized so that the sum of powers of all the modes is equal to unity. Fig. 3 shows a representation of DMD mode powers and how it differs between seizure and seizure-free regions for two EEG recordings from Patient 1 of the CHB-MIT dataset. It can be seen how the values of normalized DMD powers, accumulated on discretized bins of width 4 Hz, differ significantly in the two scenarios, with seizure regions having much higher concentration of power in the lower end of the spectrum, i.e., in the frequency interval from 0 Hz to 16 Hz.

Curve-length (l_c) serves as an indirect measure of the amplitude and variation of the time domain EEG signal. For the n-th channel of the EEG signal, the curve length $l_c(n)$ can be computed as

$$l_c(n) = \sum_{k=0}^{m-2} \sqrt{(\mathbf{X}_{n,k+1} - \mathbf{X}_{n,k})^2 + \Delta t^2}, \qquad (6)$$
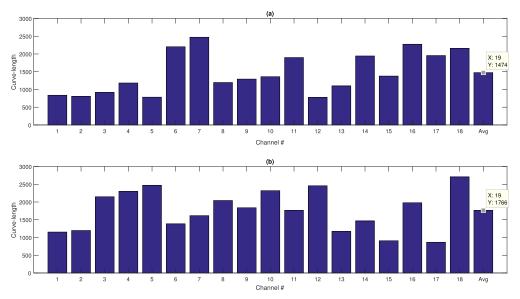
FIGURE 4. (a) Channel-wise and average curve-lengths for non-seizure epoch shown in Fig 1a, (b) Channel-wise and average curve-lengths for seizure epoch shown in Fig 1d.

where m is the sampling frequency and Δt is the sampling interval. Curve-length is calculated for each 1-second epoch of each channel of the data (18 channels for CHB-MIT dataset and 22 channels for KU Leuven dataset). Fig. 4 shows the comparison of curve-lengths for EEG signal epochs selected from recordings of Patient 1 in CHB-MIT dataset. Each of the epochs are representative of seizure and non-seizure regions. The curves lengths are generally larger for the channels in the seizure region as compared to the corresponding curve lengths in the non-seizure region. This fact is also emphasized by the curve-lengths averaged across all the EEG channels, which is depicted in the rightmost bar in both subplots of Fig. 4. This demonstrates the effectiveness of curve-length as a feature that can distinguish between seizure and non-seizure epochs. So, the individual curve-lengths of the channels along with the mode powers in each bins are employed as features for the proposed approach. As a result of this choice, the dimension of the feature vector for the proposed method is 50 (and 54) for the CHB-MIT data-set (and KU Leuven data), respectively. It should be mentioned that the curve length averaged across channels is not used in the proposed approach for classification, as it is dependent upon the individual curve lengths of the channels.

While this work primarily depends upon the use of spatio-temporal DMD modes for seizure detection, the curve-length feature plays a complementary role by providing additional temporal information about the EEG signal. It was observed that the addition of curve-length as a feature has little effect on the sensitivity, but it improves the specificity by around 2% without incurring any significant computational cost.

C. CLASSIFICATION
The CHB-MIT dataset contains two kinds of recordings, seizure-free (only non-ictal activity) and those containing one or more seizures, i.e., both ictal and non-ictal regions.

TABLE 1. CHB-MIT dataset split between training and testing sets.

Patient	Training Data Duration (s)		Test Data Duration (s)	
	Non-seizure	Seizure	Non-seizure	Seizure
Patient1	74442	221	71104	221
Patient2	64710	90	62077	82
Patient3	68196	204	68208	198
Patient4	280295	160	281161	218
Patient5	68089	321	68163	237
Patient6	99604	84	140489	69
Patient7	113935	182	127128	143
Patient8	31946	454	39158	465
Patient9	123087	150	120975	126
Patient10	93435	228	86202	219
Patient11	64744	54	59707	752
Patient13	60936	264	57329	271
Patient14	46715	85	46716	84
Patient15	78222	989	63822	1003
Patient16	28755	45	39561	39
Patient17	39446	178	35885	115
Patient18	64642	169	63326	148
Patient19	53857	155	53653	81
Patient20	50288	136	48784	158
Patient21	56884	106	61106	93
Patient22	57481	130	53926	74
Patient23	45542	244	49644	180
Patient24	39353	247	36803	264
Total	**1704604**	**4896**	**1734927**	**5240**

Roughly half of the seizure-free recordings were used for training/validation, while the other half were used for testing. Recordings containing the seizure activity were split such that duration of seizures in both data portions, i.e., those employed for testing and training, was nearly equal. It was ensured that no recording was split such that its different portions were in both training and testing data. This was done to ensure the classifier had no bias to any recording. Table 1 shows the distribution of data into training and testing segments.

In case of KU Leuven dataset, n-fold cross validation was employed, where $n = 27$ is the total number of recordings. For each test, the other $n-1$ recordings were used to train the classifier. Although the data from same patient was used to

train the classifier, there was no overlap of testing and training data at any stage.

Since the data distribution in cases such as seizure detection is highly imbalanced, i.e., the number of samples of one class are much less than the other class(es), most of the traditionally used classifiers do not generate promising results. Such imbalances can be improved using two techniques: data sampling and boosting [46]. The former improves the class balance by either adding samples of the smaller class (oversampling) or removing samples of the larger class (under-sampling) while the latter is an iterative approach that improves performance by converting weak learners to strong ones. The most popular boosting algorithm, namely AdaBoost, boosts the strength of learners by initially building an iterative ensemble of models. At each iteration, AdaBoost aims to correctly classify those samples, in the next iteration by adjusting weights, which were incorrectly classified in the current iteration [47]. RUSBoost [48] is a hybrid approach inspired by AdaBoost that uses a combination of sampling and boosting. We use RUSBoost in this study to address the data imbalance issue inherent in epileptic EEG data. RUSBoost performs random under-sampling of the majority class before building an ensemble of classifiers that provides comparable performance with more complicated hybrid algorithms, e.g., SMOTEBoost [49]. The high-dimensional nature and imbalanced distribution of EEG data make RUSBoost algorithm an ideal candidate for seizure detection.

D. POST-PROCESSING
The transition of neural activity from non-seizure state to seizure state is not entirely sudden, and may take several epochs. Therefore, certain post-processing is required to aggregate the outcomes of several epoch to decide on the presence or absence of a seizure. A study conducted on over 150 patients shows that the median length of various types of seizures ranges from 18 seconds to 130 seconds [50].

This allows us to use the following post-processing measures in our work:

1) A run-length smoothing filter that predicts a seizure only if the classifier predicts one for ten consecutive epochs [51]. The run-length smoothing filter ensures no isolated false detection are carried forward, hence reducing the number of false alarms. The smoothing may adversely affect the sensitivity of the algorithm if the actual length of the seizure is less than that of the filter.
2) Detections are grouped together for 60 epochs [52]. The grouping is used to avoid over-representation of positive detections. Theoretically, it may misrepresent the number of seizures detected if multiple seizures occur in a single 60-second window.

V. RESULTS AND DISCUSSION
To evaluate the performance of the proposed algorithm, the universally accepted metrics of specificity and sensitivity are used. The terms are defined as follows:

A *positive detection* occurs when the algorithm flags the presence of a seizure.

A *true positive* (TP) is counted when the *positive detection* by the algorithm coincides with the interval marked as seizure by the human expert. To cater for the ambiguity in seizure onset/offset times, TP is reported if *positive detection* occurs anytime between 1 minute before onset and 1 minute after the end of the seizure.

A *false positive* (FP) is reported when a positive detection occurs outside the seizure window, which consists of the seizure, 3 minutes of pre-seizure activity, and 3 minutes of post-seizure activity. This 3 minute time frame is excluded so that epileptic activities, frequently serving as precursors to a seizure, are not counted as FPs [52].

A *true negative* (TN) is a seizure free region reported correctly by the proposed algorithm.

A *false negative* (FN) is a seizure that the algorithm fails to detect. Using these definitions, we calculate the following performance evaluation metrics:

- *True Positive Rate* or *Sensitivity* provide the probability of correct detection of seizure. It is calculated as

$$\text{Sensitivity} = \text{TPR} = \frac{\text{\# of TPs}}{\text{\# of seizures}} \qquad (7)$$

- *True Negative Rate* or *Specificity* provides the probability of correct identification of seizure-free region. It is calculated as:

$$\text{Specificity} = \text{TNR} = \frac{\text{\# of TNs}}{\text{\# of TNs} + \text{\# of FPs}} \qquad (8)$$

- *False Positive Rate per hour* is the average number of false alarms reported in an hour.
- *Onset Latency* is the delay in the detection of seizure by the algorithm as compared to the ground truth marked by clinician.

A. CHB-MIT DATASET
CHB-MIT dataset contains 661 recordings from 23 patients containing a total of 158 seizures in around 958 hours of EEG data (excluding patient 12). The classifiers are patient-specific, i.e., they are trained on their respective training data. Although the type of classifier is the same for all patients, i.e., RUSBoost decision trees, the parameters, (i.e., the number of learners, learning rate, and the number of splits) have been chosen to get best results on per-patient basis.

The results for performance metrics are reported in Table 2 with weighted averages of all mentioned at the bottom.

The weights are according to total number of seizures and epochs for each patient. It can be seen that sensitivity is close to 1, if not exactly 1, for most patients. The worst sensitivity is obtained for Patient 16. The reason for poor performance is due to the post-processing step of the proposed algorithm. For Patient 16, 4 out of 5 test seizures have duration $< 10s$, which cannot be flagged as a true positive by our algorithm due to the 10-second run length smoothing applied during post-processing. If this particular patient is not included
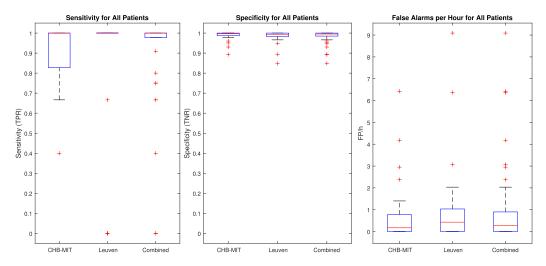
FIGURE 5. Box plots for Sensitivity, Specificity, and False Alarms per hour on CHB-MIT and KU Leuven Datasets.

TABLE 2. Results - CHB MIT dataset.

Patient	No. of Test Seizures	TPR	TNR	FPR/h
Patient1	3	1	1	0
Patient2	1	1	0.9923	0.4642
Patient3	3	1	0.9303	4.1799
Patient4	2	1	0.9998	0.0128
Patient5	2	1	1	0
Patient6	5	0.8	0.9991	0.0514
Patient7	1	1	1	0
Patient8	3	1	0.9908	0.5547
Patient9	2	1	1	0
Patient10	3	1	1	0
Patient11	1	1	1	0
Patient13	4	0.75	0.8929	6.4263
Patient14	4	0.75	0.9508	2.9495
Patient15	11	0.9091	0.9858	0.8539
Patient16	5	0.4	0.9603	2.3817
Patient17	1	1	0.9766	1.4023
Patient18	3	0.6667	0.9971	0.1711
Patient19	1	1	0.9989	0.0673
Patient20	4	0.75	0.9975	0.1485
Patient21	2	1	0.9970	0.1772
Patient22	1	1	1	0
Patient23	3	1	0.9951	0.2920
Patient24	6	1	0.9927	0.4390
W. Avg		**0.8732**	**0.9893**	**0.6412**

TABLE 3. Results - KU Leuven dataset.

Patient	No. of Test Seizures	TPR	TNR	FPR/h
Patient1	1	1	0.9900	0.6012
Patient2	1	1	1	0
Patient3	1	1	0.9919	0.4878
Patient4	1	1	0.9938	0.3738
Patient5	1	1	0.9901	0.5941
Patient6	1	0	1	0
Patient7	1	1	0.9890	0.6593
Patient8	1	0	1	0
Patient9	1	1	1	0
Patient10	1	1	1	0
Patient11	1	0	0.9828	1.0345
Patient12	1	1	0.9674	1.9565
Patient13	1	1	0.8485	9.0909
Patient14	2	1	1	0
Patient15	1	1	0.9661	2.0339
Patient16	1	1	0.9489	3.0682
Patient17	5	1	0.9914	0.5161
Patient18	3	1	1	0
Patient19	1	1	0.9986	0.0820
Patient20	2	1	0.9960	0.2381
Patient21	3	0.6667	0.8939	6.3673
Patient22	1	1	0.9953	0.2810
W. Avg		**0.875**	**0.9884**	**0.6941**

in the performance analysis, the sensitivity increases from 0.87 to 0.91.

Our algorithm provides performance comparable to that of Shoeb and Guttag [6]. For instance, we have a sensitivity of 87% as opposed to 96% and a median false alarm rate of $4/24hr$ compared to $2/24hr$ given in [6]. However, the proposed algorithm provides this performance using only spectral (DMD mode powers) and temporal (curve-length) features while Shoeb et al. also used spatial and non-EEG features in their algorithm, such as electro-cardiogram (ECG) signal.

B. KU LEUVEN EEG DATA

KU Leuven dataset contains 27 recordings from 22 patients containing a total of 32 seizures in around 110 hours of EEG

recordings. Table 3 represents the results for KU Leuven dataset. The methodology is same as the one used for CHB-MIT dataset, except that we use 15 second run-length smoothing instead of the 10 second smoothing applied in the previous case. This is done to combat the relatively large number of false alarms at the expense of sensitivity which falls from 0.93 to 0.88. It can be seen from the table that the worst performance of the algorithm, in terms of false alarm rate, is for Patient 21. If we exclude it from the analysis, the false alarm rate drops to $0.54/hr$ which is of the same order as provided in [22]. In case of KU Leuven dataset, our algorithm shows higher sensitivity (88% as compared to 84%) at the cost of a slightly higher false alarm rate compared to the work of Hunyadi *et al.* [22].

Fig. 5 shows the box-plots of sensitivity, specificity and false alarms per hour values of CHB-MIT and KU Leuven

datasets. It can be seen that the values of sensitivity and specificity are generally close to 1 while the occurrence of false alarms per hour is generally low.

C. LIMITATIONS AND FUTURE DIRECTIONS

We have observed that the proposed approach achieves good sensitivity by using the features primarily derived from the spatio-temporal modes of DMD. Considering the noisy nature of scalp EEG, the proposed algorithm is robust and indicates its utility for miscellaneous applications, such as brain-computer interfaces, P-300 oddball paradigm among others. Further improvement in false alarm rate could be achieved if auxiliary features such as mean, variance, skewness, etc., are included. Another future direction could be the use of recently developed multi-resolution dynamic mode decomposition [41] to further reduce the false alarm rate.

VI. CONCLUSIONS

This paper presented dynamic mode decomposition (DMD), an algorithm that captures the spatio-temporal characteristics of multi-channel signals, and demonstrated its applicability to the epileptic seizure detection from the scalp EEG recordings. The proposed approach employed power of the DMD modes and the curve-length of the EEG signal to train and test classifiers on two large scalp EEG datasets. The performance assessment of the proposed algorithm indicated that DMD effectively captures the dynamics of EEG signals and is capable of distinguishing between seizure and non-seizure portions of scalp EEG recordings.

REFERENCES

[1] *Epilepsy—World Health Organization Fact Sheet*. [Online]. Available: http://www.who.int/mediacentre/factsheets/fs999/en

[2] E. Niedermeyer and d. S. F. Lopes, *Electroencephalography: Basic Principles, Clinical Applications, and Related Fields*. Philadelphia, PA, USA: Lippincott Williams and Wilkins, 2005.

[3] S. B. Wilson, M. L. Scheuer, C. Plummer, B. Young, and S. Pacia, "Seizure detection: Correlation of human experts," *Clin. Neurophysiol.*, vol. 114, no. 11, pp. 2156–2164, 2003.

[4] A. B. Gardner, A. M. Krieger, G. Vachtsevanos, and B. Litt, "One-class novelty detection for seizure analysis from intracranial EEG," *J. Mach. Learn. Res.*, vol. 7, pp. 1025–1044, Jun. 2006.

[5] S. Grewal and J. Gotman, "An automatic warning system for epileptic seizures recorded on intracerebral EEGs," *Clin. Neurophysiol.*, vol. 116, no. 10, pp. 2460–2472, 2005.

[6] A. H. Shoeb and J. V. Guttag, "Application of machine learning to epileptic seizure detection," in *Proc. Int. Conf. Mach. Learn.*, 2010, pp. 975–982.

[7] A. L. Goldberger *et al.*, "Physiobank, physiotoolkit, and physionet," *Circulation*, vol. 101, no. 23, pp. 215–220, 2000.

[8] C.-Y. Chiang, N.-F. Chang, T.-C. Chen, H.-H. Chen, and L.-G. Chen, "Seizure prediction based on classification of EEG synchronization patterns with on-line retraining and post-processing scheme," in *Proc. Int. Conf. Eng. Med. Biol. Soc.*, 2011, pp. 7564–7569.

[9] S. Kiranyaz, T. Ince, M. Zabihi, and D. Ince, "Automated patient-specific classification of long-term electroencephalography," *J. Biomed. Inf.*, vol. 49, pp. 16–31, Jun. 2014.

[10] S. Kiranyaz, T. Ince, A. Yildirim, and M. Gabbouj, "Evolutionary artificial neural networks by multi-dimensional particle swarm optimization," *Neural Netw.*, vol. 22, no. 10, pp. 1448–1462, 2009.

[11] N. Ahammad, T. Fathima, and P. Joseph, "Detection of epileptic seizure event and onset using EEG," *BioMed Res. Int.*, vol. 2014, Nov. 2014, Art. no. 450573.

[12] M. A. Ahmad *et al.*, "Comparative analysis of classifiers for developing an adaptive computer-assisted EEG analysis system for diagnosing epilepsy," *BioMed Res. Int.*, vol. 2015, Jan. 2015, Art. 638036.

[13] S. Bugeja, L. Garg, and E. E. Audu, "A novel method of EEG data acquisition, feature extraction and feature space creation for early detection of epileptic seizures," in *Proc. Int. Conf. Eng. Med. Biol. Soc.*, 2016, pp. 837–840.

[14] A. Bhattacharyya and R. B. Pachori, "A multivariate approach for patient-specific eeg seizure detection using empirical wavelet transform," *IEEE Trans. Biomed. Eng.*, vol. 64, no. 9, pp. 2003–2015, Sep. 2017.

[15] A. Supratak, L. Li, and Y. Guo, "Feature extraction with stacked autoencoders for epileptic seizure detection," in *Proc. Int. Conf. Eng. Med. Biol. Soc.*, 2014, pp. 4184–4187.

[16] M. Z. Ahmad, A. M. Kamboh, S. Saleem, and A. A. Khan, "Mallat's scattering transform based anomaly sensing for detection of seizures in scalp EEG," *IEEE Access*, vol. 5, pp. 16919–16929, 2017.

[17] P. Fergus, D. Hignett, A. Hussain, D. Al-Jumeily, and K. Abdel-Aziz, "Automatic epileptic seizure detection using scalp EEG and advanced artificial intelligence techniques," *BioMed Res. Int.*, vol. 2015, Dec. 2015, Art. no. 986736.

[18] J. Xiang *et al.*, "The detection of epileptic seizure signals based on fuzzy entropy," *J. Neurosci. Methods*, vol. 243, pp. 18–25, Mar. 2015.

[19] M. Zabihi, S. Kiranyaz, A. B. Rad, A. K. Katsaggelos, M. Gabbouj, and T. Ince, "Analysis of high-dimensional phase space via Poincaré section for patient-specific seizure detection," *IEEE Trans. Neural Syst. Rehabil. Eng.*, vol. 24, no. 3, pp. 386–398, Mar. 2016.

[20] M. H. Myers, A. Padmanabha, G. Hossain, A. L. de Jongh Curry, and C. D. Blaha, "Seizure prediction and detection via phase and amplitude lock values," *Frontiers Human Neurosci.*, vol. 10, p. 80, Mar. 2016.

[21] C. Zhang, M. A. B. Altaf, and J. Yoo, "Design and implementation of an on-chip patient-specific closed-loop seizure onset and termination detection system," *IEEE J. Biomed. Health Inform.*, vol. 20, no. 4, pp. 996–1007, Jul. 2016.

[22] B. Hunyadi, M. De Vos, W. Van Paesschen, and S. Van Huffel, "A mimicking approach for human epileptic seizure detection," in *Proc. Int. Biosignal Process. Conf.*, 2010, pp. 1–4.

[23] R. G. Andrzejak, K. Lehnertz, F. Mormann, C. Rieke, P. David, and C. E. Elger, "Indications of nonlinear deterministic and finite-dimensional structures in time series of brain electrical activity: Dependence on recording region and brain state," *Phys. Rev. E, Stat. Phys. Plasmas Fluids Relat. Interdiscip. Top.*, vol. 64, no. 6, p. 061907, 2001.

[24] R. B. Pachori, "Discrimination between ictal and seizure-free EEG signals using empirical mode decomposition," *Res. Lett. Signal Process.*, vol. 2008, Dec. 2008, Art. no. 293056.

[25] R. B. Pachori and V. Bajaj, "Analysis of normal and epileptic seizure EEG signals using empirical mode decomposition," *Comput. Methods Programs Biomed.*, vol. 104, no. 3, pp. 373–381, 2011.

[26] V. Bajaj and R. B. Pachori, "Classification of seizure and nonseizure EEG signals using empirical mode decomposition," *IEEE Trans. Inf. Technol. Biomed.*, vol. 16, no. 6, pp. 1135–1142, Nov. 2012.

[27] R. B. Pachori and S. Patidar, "Epileptic seizure classification in EEG signals using second-order difference plot of intrinsic mode functions," *Comput. Methods Programs Biomed.*, vol. 113, no. 2, pp. 494–502, 2014.

[28] V. Joshi, R. B. Pachori, and A. Vijesh, "Classification of ictal and seizure-free EEG signals using fractional linear prediction," *Biomed. Signal Process. Control*, vol. 9, pp. 1–5, Jan. 2014.

[29] A. K. Tiwari, R. B. Pachori, V. Kanhangad, and B. K. Panigrahi, "Automated diagnosis of epilepsy using key-point-based local binary pattern of EEG signals," *IEEE J. Biomed. Health Inform.*, vol. 21, no. 4, pp. 888–896, Jul. 2017.

[30] D. Bhati, M. Sharma, R. B. Pachori, and V. M. Gadre, "Time–frequency localized three-band biorthogonal wavelet filter bank using semidefinite relaxation and nonlinear least squares with epileptic seizure EEG signal classification," *Digit. Signal Process.*, vol. 62, pp. 259–273, Mar. 2017.

[31] A. Bhattacharyya, R. B. Pachori, A. Upadhyay, and U. R. Acharya, "Tunable-Q wavelet transform based multiscale entropy measure for automated classification of epileptic EEG signals," *Appl. Sci.*, vol. 7, no. 4, p. 385, 2017.

[32] M. Sharma, R. B. Pachori, and U. R. Acharya, "A new approach to characterize epileptic seizures using analytic time-frequency flexible wavelet transform and fractal dimension," *Pattern Recognit. Lett.*, vol. 94, pp. 172–179, Jul. 2017.

[33] M. Sharma and R. B. Pachori, "A novel approach to detect epileptic seizures using a combination of tunable-Q wavelet transform and fractal dimension," *J. Mech. Med. Biol.*, vol. 17, no. 7, p. 1740003, 2017.

[34] D. Bhati, R. B. Pachori, and V. M. Gadre, "A novel approach for time–frequency localization of scaling functions and design of three-band biorthogonal linear phase wavelet filter banks," *Digit. Signal Process.*, vol. 69, pp. 309–322, Oct. 2017.

[35] R. R. Sharma and R. B. Pachori, "Time–frequency representation using IEVDHM–HT with application to classification of epileptic EEG signals," *IET Sci., Meas. Technol.*, vol. 12, no. 1, pp. 72–82, 2018.

[36] P. J. Schmid, "Dynamic mode decomposition of numerical and experimental data," *J. Fluid Mech.*, vol. 656, pp. 5–28, Jan. 2010.

[37] P. J. Schmid, L. Li, M. P. Juniper, and O. Pust, "Applications of the dynamic mode decomposition," *Theor. Comput. Fluid Dyn.*, vol. 25, no. 1, pp. 249–259, 2011.

[38] K. K. Chen, J. H. Tu, and C. W. Rowley, "Variants of dynamic mode decomposition: Boundary condition, Koopman, and fourier analyses," *J. Nonlinear Sci.*, vol. 22, no. 6, pp. 887–915, 2012.

[39] A. Wynn, D. Pearson, B. Ganapathisubramani, and P. Goulart, "Optimal mode decomposition for unsteady flows," *J. Fluid Mech.*, vol. 733, p. 473, 2013.

[40] J. H. Tu, C. W. Rowley, D. M. Luchtenburg, S. L. Brunton, and J. N. Kutz. (2013). "On dynamic mode decomposition: Theory and applications." [Online]. Available: https://arxiv.org/abs/1312.0041

[41] J. N. Kutz, X. Fu, and S. L. Brunton, "Multiresolution dynamic mode decomposition," *SIAM J. Appl. Dyn. Syst.*, vol. 15, no. 2, pp. 713–735, 2016.

[42] B. W. Brunton, L. A. Johnson, J. G. Ojemann, and J. N. Kutz, "Extracting spatial–temporal coherent patterns in large-scale neural recordings using dynamic mode decomposition," *J. Neurosci. Methods*, vol. 258, pp. 1–15, Jan. 2016.

[43] J. N. Kutz, *Data-Driven Modeling & Scientific Computation: Methods for Complex Systems & Big Data*, 1st ed. Oxford, U.K.: Oxford Univ. Press, 2013.

[44] C. W. Rowley, I. Mezić, S. Bagheri, P. Schlatter, and D. S. Henningson, "Spectral analysis of nonlinear flows," *J. Fluid Mech.*, vol. 641, pp. 115–127, Dec. 2009.

[45] M. Gavish and D. L. Donoho, "The optimal hard threshold for singular values is $4/\sqrt{3}$," *IEEE Trans. Inf. Theory*, vol. 60, no. 8, pp. 5040–5053, Aug. 2014.

[46] G. M. Weiss, "Mining with rarity: A unifying framework," *ACM SIGKDD Explorations Newslett.*, vol. 6, no. 1, pp. 7–19, Jun. 2004.

[47] Y. Freund and R. E. Schapire, "Experiments with a new boosting algorithm," in *Proc. Int. Conf. Mach. Learn.*, vol. 96. 1996, pp. 148–156.

[48] C. Seiffert, T. M. Khoshgoftaar, J. Van Hulse, and A. Napolitano, "RUSBoost: Improving classification performance when training data is skewed," in *Proc. Int. Conf. Pattern Recognit.*, 2008, pp. 1–4.

[49] N. V. Chawla, A. Lazarevic, L. O. Hall, and K. W. Bowyer, "Smoteboost: Improving prediction of the minority class in boosting," in *Proc. Eur. Conf. Princ. Data Mining Knowl. Discovery*. Berlin, Germany: Springer, 2003, pp. 107–119.

[50] S. Jenssen, E. J. Gracely, and M. R. Sperling, "How long do most seizures last? A systematic comparison of seizures recorded in the epilepsy monitoring unit," *Epilepsia*, vol. 47, no. 9, pp. 1499–1503, 2006.

[51] L. Orosco, A. G. Correa, P. Diez, and E. Laciar, "Patient non-specific algorithm for seizures detection in scalp EEG," *Comput. Biol. Med.*, vol. 71, pp. 128–134, Apr. 2016.

[52] A. Varsavsky, I. Mareels, and M. Cook, *Epileptic Seizures and the EEG: Measurement, Models, Detection and Prediction*. Boca Raton, FL, USA: CRC Press, 2011.

MUHAMMAD SOHAIB J. SOLAIJA (S'16) received the master's degree in electrical engineering from the National University of Sciences and Technology. His research interests lie in digital signal processing and its applications in biomedical sensing and communications.

SAJID SALEEM (S'09–M'14) received the B.Sc. degree in electrical engineering from the National University of Sciences and Technology, Islamabad, Pakistan, in 2006, and the M.S. degree in mathematics and the Ph.D. degree in electrical and computer engineering from the Georgia Institute of Technology, Atlanta, GA, USA, in 2011 and 2013, respectively. Since 2014, he has been an Assistant Professor with the School of Electrical Engineering and Computer Science, National University of Sciences and Technology. His research interests include signal processing for biomedical engineering and communications, brain–computer interfaces, and time-frequency analysis.

KHAWAR KHURSHID received the Ph.D. degree in biomedical imaging systems from Michigan State University. He is currently Heading the Institute of Applied Electronics and Computers, National University of Sciences and Technology, Pakistan. He is also the Director of the Center of Excellence in FPGA and ASIC Research. He specializes in medical imaging, embedded systems, pattern recognition, image and signal processing with research interests in the areas of wearable devices, image segmentation, registration, video encoding, multimedia streaming, and 3-D display systems.

SYED ALI HASSAN (S'07–M'12–SM'17) received the B.E. degree (Hons.) in electrical engineering from the National University of Sciences and Technology (NUST), Pakistan, in 2004, the M.S. degree in electrical engineering from the University of Stuttgart, Germany, in 2007, and the M.S. degree in mathematics and the Ph.D. degree in electrical engineering from the Georgia Institute of Technology, Atlanta, GA, USA, in 2011. He was a Research Associate with Cisco Systems Inc., San Jose, CA, USA. He is currently an Assistant Professor with the School of Electrical Engineering and Computer Science (SEECS), NUST, where he is also the Director of the Information Processing and Transmission Research Group, which focuses on various aspects of theoretical communications. He has co-authored over 100 publications in international conferences and journals. His broader area of research is signal processing for communications. He has served as a TPC Member for the IEEE VTC Spring 2013, the IEEE PIMRC 2013–2014, the IEEE WCSP 2014, and MILCOM 2014–2016.

AWAIS MEHMOOD KAMBOH (S'06–M'11–SM'17) received the B.E. degree in electrical engineering from the National University of Sciences and Technology, Islamabad, Pakistan, in 2003, the M.S. degree in electrical engineering (systems) from the University of Michigan, Ann Arbor, MI, USA, in 2006, and the Ph.D. degree in electrical engineering from Michigan State University, East Lansing, MI, USA, in 2010. Since 2011, he has been an Assistant Professor with the School of Electrical Engineering and Computer Science (SEECS), National University of Sciences and Technology, Islamabad, Pakistan. He is also the Director of the Neuroinformatics Research Lab and the Analog Mixed Signal Research Lab at SEECS. His research interests include mixed-signal integrated-circuits, biomedical signal processing, and brain–computer interfaces.

• • •